Available online at www.sciencedirect.com
ScienceDirect
Lithos 95 (2007) 267–278
LITHOS
www.elsevier.com/locate/lithos

Flat rare earth element patterns as an indicator of cumulate processes in the Lesser Qinling carbonatites, China

Cheng Xu [a,b,*], Ian H. Campbell [b], Charlotte M. Allen [b], Zhilong Huang [a], Liang Qi [c], Huan Zhang [a], Guishan Zhang [a]

[a] *Laboratory of Materials of the Earth's Interior and Geofluid Processes, Institute of Geochemistry, Chinese Academy of Sciences, Guiyang 550002, China*
[b] *Research School of Earth Sciences, Australian National University, Canberra, Australia*
[c] *Department of Earth Sciences, University of Hong Kong, Hong Kong, China*

Received 24 November 2005; accepted 14 July 2006
Available online 28 August 2006

Abstract

The Lesser Qinling carbonatite dykes are mainly composed of calcites. They are characterized by unusually high heavy rare earth element concentrations (HREE; e.g. Yb > 30 ppm) and flat to weakly light rare earth element (LREE) enriched chondrite-normalized patterns ($La/Yb_n = 1.0–5.5$), which is in marked contrast with all other published carbonatite data. The trace element contents of calcite crystals were measured in situ by laser ablation inductively coupled plasma mass spectrometry (LA-ICPMS). Some crystals show reduced LREE from core to rim, whereas their HREE compositions are relatively constant. The total REE contents and chondrite-normalized REE patterns from the cores of carbonate crystals are similar to those of the whole rock. The carbon and oxygen isotopic compositions of calcites fall within the range of primary, mantle-derived carbonatites. The initial Sr isotopic compositions (0.70480–0.70557) of calcites are consistent with an EM1 source or mixing between HIMU and EM1 mantle sources. However these sources cannot produce carbonatite parental magmas with a flat or slightly LREE enrichment pattern by low degrees of partial melting. Analyses of carbonates from other carbonatites show that carbonates have nearly flat REE pattern if they crystallize from a LREE enriched carbonatite melt. This implies that when carbonates crystallize from a carbonatite melt the calcite/melt partition coefficients (D) for HREE are much greater than the D for the LREE. The nearly flat REE patterns of the Lesser Qinling carbonatites can be explained if they are carbonate cumulates that contain little trapped carbonatite melt. Strong enrichment of HREE in the carbonatites may require their derivation by small degrees of melting from a garnet-poor source.

Keywords: Carbonatites; Rare earth elements; Crystal cumulates; Lesser Qinling

1. Introduction

Carbonatites are mantle-derived magmatic rocks that intrude both continental and oceanic crusts. They are typically characterized by very high concentrations of light rare earth (LREE) and other highly incompatible trace elements (e.g. Sr, Ba). The origin of carbonatites has been extensively debated. There are three principal hypotheses: (1) direct melting of a carbonate-bearing mantle source (Harmer and Gittins, 1998; Harmer, 1999), (2) generation as immiscible liquids from a CO_2-rich silicate magmas (Kjarsgaard and Hamilton, 1989; Lee and Wyllie, 1997a,b), (3) products of extensive crystal fractionation from a CO_2-

* Corresponding author. Present address: Institute of Geochemistry, Chinese Academy of Science, 73 Guanshui Road, Guiyang 550002, Guizhou Province, China. Tel.: +86 851 5891117.
E-mail address: xucheng1999@hotmail.com (C. Xu).

0024-4937/$ - see front matter © 2006 Elsevier B.V. All rights reserved.
doi:10.1016/j.lithos.2006.07.016

rich silicate magma (Veksler et al., 1998a; Verhulst et al., 2000). Although ample experiments have shown that carbonatites can be produced in different ways, there are no robust criteria that can be used to separate primary carbonatitic melts from those produced by differentiation of a parent silicate melt (Bell, 1998). In addition, most carbonatites that are seen at crustal levels are end-products of a complex evolution of primary mantle-derived melts that may involve crystal cumulates and loss of fluids and volatiles (Le Bas, 1989; Lee and Wyllie, 1998). Relating observed upper crustal carbonatites to primary carbonatite composition is not always straightforward.

The Qinling orogenic belt separates the North China block from the South China block, and is critical for unraveling the tectonic history of East Asia (Fig. 1). The Lesser Qinling is located in the northernmost Qinling orogenic belt. Three carbonatite dykes were intruded in this area, which can potentially provide information about the mantle that underlies this critical region in China. However, the Lesser Qinling samples are not typical carbonatites and do not strongly show LREE enrichment. Their whole rock analyses are characterized by high HREE contents and flat to slightly LREE enrichment patterns, which requires either that they formed by a mantle process that is different to other carbonatites or that their geochemical characteristics are not representative of the primary mantle-derived carbonatite.

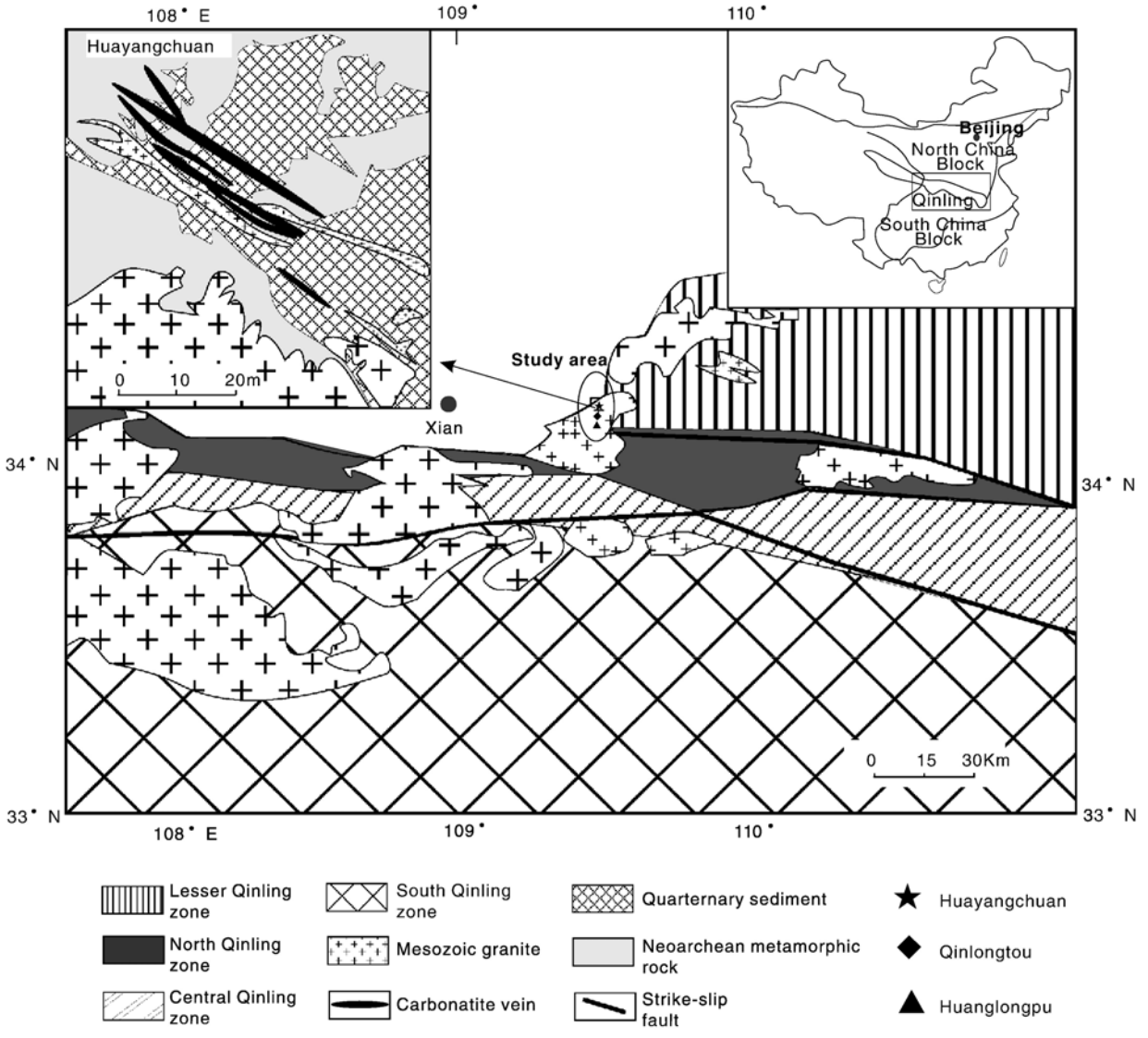

Fig. 1. Geological sketch of the Qinling orogenic belt and detailed map of the Huayangchuan carbonatite dyke (modified after Yu, 1992; Xue et al., 1996).

In this paper we report major and trace element chemistry and C–O–Sr isotopic data for the Lesser Qinling carbonatites. We show that the trace element compositions of whole rock carbonatites, obtained by solution ICPMS, are similar to that of the carbonate minerals as determined in situ by LA-ICPMS. We argue that this is only possible if the carbonatites are cumulates so that the chemistry of the rocks is controlled by the chemistry of the carbonate minerals and therefore is not representative of the primary carbonate melt.

2. Geological setting and sampling

The Qinling orogenic belt is composed of four zones separated by major faults (Xue et al., 1996). These are called the Qinling zones: South, Central, North and Lesser. The carbonatite dykes from the Lesser Qinling zone are located at the central Shanxi Province, China, including the towns of Huayangchuan (HYC), Qinlongtou (QLT) and Huanglongpu (HLP). The area is situated at the boundary between the Qinling orogenic belt and North China block (Fig. 1). The detailed geological framework and tectonic evolution of the Qinling region have been described by Xue et al. (1996), Meng and Zhang (2000), and Ratschbacher et al. (2003) but little work has been carried out on the carbonatite dykes. Detailed geological maps of the Qinlongtou and Huanglongpu are not available, but a map of Huayangchuan is provided in Fig. 1.

The main outcrop of the Lesser Qinling carbonatites occurs as dykes that cut a thrust pile of gneiss, quartzites and slates of late Archaean to Mesoproterozoic age, which are intruded by Mesozoic granites. A minor syenite is also emplaced as a dyke, but fresh samples are difficult to find because it is highly altered. The dyke is not shown in Fig. 1. Fenitization and albitization are present at the margins of the carbonatite dykes. The fenitized granites display sap green with high aegirine–augite composition. Occasionally, pegmatitic aegirine–augite is found in some of them. The only geochronology for the carbonatite dykes is from HYC, which gives a phlogopite K–Ar age of 181 Ma (Yu, 1992). These carbonatite dykes are mostly composed of coarse, generally euhedral grains of calcite (>90%), with individual crystal typically 0.8–2.6 mm in size (Fig. 2). Minor and accessory phases include microcline, aegirine–augite, arfvedsonite, phlogopite, quartz, celestite, barite, magnetite, sulphides, bastnaesite and apatite. At HLP, the rock contains minor amounts of molybdenite, and calcite is pink. Rarely, radioactive minerals, such as liandratite and thorite, are found in the HYC carbonatite dyke. At the three locations very coarse quartz is irregularly distributed at the margin of the carbonatite dyke. Field observation indicates that the quartz mass was penetrated, broken and incorporated by late emplacement of the carbonatite dyke.

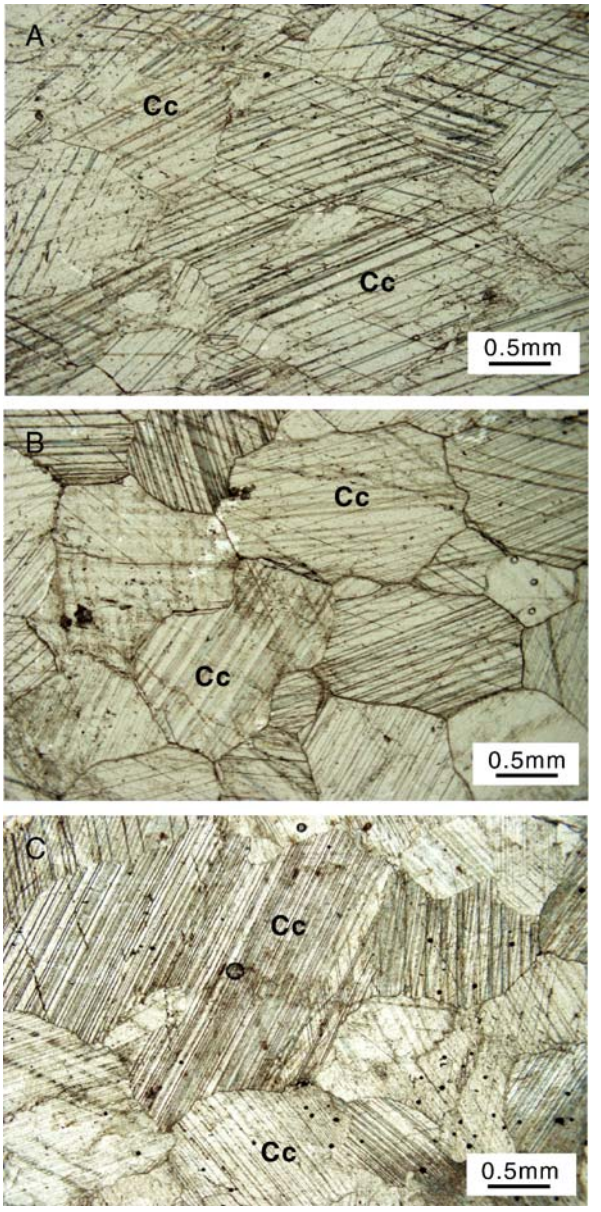

Fig. 2. Photomicrographs of the Lesser Qinling carbonatites (plane-polarized transmitted light; scale bar is 0.5 mm). Cc, calcite; A, sample HYC-7; B, sample HLP-1; C, sample QLT-1.

3. Analytical methods

The major elements of whole rock samples were determined by wet chemical methods at the Institute of Geochemistry, Chinese Academy of Sciences. Representative calcite major element compositions of samples HYC-7, 13 were measured on C-coated polished section by JEOL

Table 1
Major and trace element compositions of carbonatites and calcites

Sample	HYC-5	HYC-7	# calcite	HYC-9	HYC-10	HYC-13	# calcite	HYC-14	HYC-20	Calciocarbonatite (range)
Main elements (wt.%)										
SiO_2	1.12	0.70	0.02	0.61	1.37	0.71	0.03	1.45		0.0–8.93
TiO_2	0.07	0.06		0.03	0.11	0.05		0.12		0.0–1.09
Al_2O_3	1.56	2.10	0.03	0.68	2.52	0.38	0.05	3.62		0.01–6.89
FeO*	0.73	0.81		0.26	0.80	0.57		0.38		0.0–13.98
Fe_2O_3			0.85				0.66			
MnO	0.35	0.88	1.67	0.38	0.58	1.33	1.61	0.23		0.0–2.57
MgO	0.41	0.40	0.52	0.10	0.42	0.34	0.33	0.18		0.0–8.11
CaO	53.10	52.96	49.25	55.09	52.62	53.72	49.78	51.17		39.24–55.40
Na_2O	0.70	0.09	0.06	0.30	0.20	0.05	0.03	0.28		0.0–1.73
K_2O	0.08	0.06	0.16	0.03	0.09	0.02	0.09	0.06		0.0–1.47
P_2O_5	0.03	0.02		0.03	0.04	0.02		0.03		0.0–10.41
CO_2	41.57	41.77		42.14	40.96	42.60		42.14		11.02–47.83
Total	99.72	99.85		99.65	99.71	99.79		99.66		
Trace elements (ppm)										
Rb	1.14	2.33		0.19	1.36	0.76		0.37	0.50	4–35
Ba	247	832		275	3269	551		2379	1227	0–45000
Th	0.94	0.14		0.91	1.14	0.11		0.24	0.46	5–168
U	0.58	0.13		24.2	0.94	0.20		0.75	0.79	0.3–29
Nb	1.71	0.67		1.62	3.24	0.66		0.65	3.39	1–15000
Ta	0.39	0.29		0.22	0.17	0.15		0.14	0.18	
Pb	115	101		107	120	103		111	129	30–108
Sr	6430	8209		10960	7436	8531		7045	7608	0–28000
Zr	2.05	0.21		0.25	2.57	0.33		0.59	0.36	4–2320
Hf	0.43	0.45		0.29	0.36	0.23		0.31	0.42	
Y	411	581		447	345	374		378	484	25–346
La	186	143		143	231	107		262	187	90–1600
Ce	522	478		545	581	401		694	571	74–4152
Pr	61.1	61.6		59.1	62.1	42.0		75.1	66.4	50–389
Nd	266	289		278	244	193		332	308	190–1550
Sm	62.9	74.7		68.7	49.6	45.5		69.3	78.3	95–164
Eu	17.9	21.3		18.5	14.6	12.3		19.7	21.8	29–48
Gd	58.5	68.5		58.6	52.7	41.8		61.7	66.1	91–119
Tb	9.24	11.6		8.35	7.62	6.36		8.32	11.1	9–10
Dy	53.9	71.8		46.1	43.5	38.4		44.9	63.9	22–46
Ho	11.7	15.5		9.64	9.20	8.69		10.2	13.1	3–9
Er	37.4	51.3		29.1	29.2	27.5		36.7	42.5	
Tm	5.99	8.28		4.36	4.96	4.43		5.90	6.64	
Yb	38.3	49.3		28.0	33.6	31.4		36.1	40.9	1.5–12
Lu	6.11	8.28		3.90	5.67	4.74		5.52	6.31	
La/Yb_n	3.31	1.97		3.45	4.66	2.32		4.93	3.11	
Gd/Yb_n	1.24	1.12		1.69	1.27	1.08		1.38	1.31	
δCe	1.18	1.23		1.44	1.17	1.44		1.20	1.24	
δEu	0.90	0.91		0.89	0.87	0.86		0.92	0.93	

Sample	HLP-1	HLP-2	HLP-3	HLP-4	HLP-5	HLP-6	QLT-1
Main elements (wt.%)							
SiO_2	1.18		1.56	1.07	1.27	4.26	
TiO_2	0.08		0.10	0.09	0.07	0.18	
Al_2O_3	2.10		2.24	1.54	1.25	6.36	
Fe*	0.37		0.51	0.41	0.48	0.35	
MnO	1.00		2.59	1.47	1.29	1.20	
MgO	0.40		0.44	0.42	0.41	0.33	
CaO	53.35		51.39	53.01	53.03	48.41	
Na_2O	0.08		0.15	0.08	0.09	0.18	
K_2O	0.18		0.06	0.04	0.02	1.03	
P_2O_5	0.04		0.05	0.03	0.03	0.05	

Table 1 (*continued*)

Sample	HLP-1	HLP-2	HLP-3	HLP-4	HLP-5	HLP-6	QLT-1
Main elements (wt.%)							
CO_2	40.94		40.65	41.48	41.67	37.37	
Total	99.71		99.74	99.63	99.61	99.72	
Trace elements (ppm)							
Rb	2.98	13.4	0.90	0.38	0.31	5.83	1.84
Ba	912	2607	154	184	197	510	625
Th	0.77	0.41	0.24	0.05	0.17	0.58	0.55
U	0.64	0.13	0.95	0.29	0.86	0.22	3.24
Nb	1.23	1.05	0.48	0.36	0.85	0.43	2.36
Ta	0.19	0.17	0.36	0.31	0.30	0.21	1.10
Pb	66.1	125	70.2	75.7	71.6	69.4	45.5
Sr	7753	9065	6938	8441	7096	7957	9408
Zr	0.43	36.8	0.38	0.28	0.21	29.3	1.31
Hf	0.22	1.0	0.46	0.29	0.36	0.82	0.24
Y	365	339	841	426	589	421	224
La	220	147	130	279	140	186	58.8
Ce	516	466	445	764	516	527	150
Pr	47.9	46.0	46.1	76.9	53.2	52.4	20.4
Nd	200	199	210	336	240	230	94.0
Sm	41.7	42.9	58.2	71.9	60.1	50.9	24.3
Eu	11.3	11.3	17.9	18.6	17.2	13.5	8.08
Gd	38.0	38.9	61.2	60.7	56.8	45.5	24.2
Tb	5.72	5.59	11.3	8.80	9.48	6.84	4.21
Dy	34.3	33.5	77.4	49.6	59.7	41.6	28.0
Ho	8.28	7.92	19.2	10.9	13.6	9.73	6.50
Er	28.6	26.3	67.3	34.2	44.9	32.9	25.3
Tm	4.86	4.48	11.8	5.23	7.52	5.47	4.62
Yb	35.3	32.3	86.0	34.7	53.0	37.9	31.9
Lu	5.55	5.02	13.3	4.82	8.11	5.61	5.43
La/Yb_n	4.24	3.09	1.03	5.46	1.79	3.34	1.25
Gd/Yb_n	0.87	0.97	0.58	1.4	0.87	0.97	0.61
δCe	1.22	1.37	1.39	1.26	1.45	1.29	1.04
δEu	0.86	0.85	0.91	0.86	0.90	0.85	1.01

HYC, Huanyangchuan; HLP, Huanglongpu; QLT, Qinlongtou. FeO*=total Fe calculated as FeO. #=repeatedly analyzed by electron probe. The range of calciocarbonatite is from Woolley and Kempe (1989).

6400 electron probe at the Australian National University using an accelerating voltage of 15 kV and a beam current of 20 nA. Whole rock trace elements (REE included) were analyzed by solution ICPMS (VG PQ-ExCell) at the University of Hong Kong. Details are given in Qi et al. (2000). The analytical precision for most elements is generally better than 10%. In situ LA-ICPMS (HP7500 Agilent) analyses of calcite on polished thin section were performed at the Australian National University. The diameter of the ablation spot varied between 54 and 86 μm. NIST 610 glass was used as a calibration standard for all samples, with ^{43}Ca as an internal standard for quantitative analysis. Detection limits were calculated after Longerich et al. (1996). Analytical precision is ≤5% at the ppm level. In-run signal intensity for indicative trace elements was monitored during analysis to make sure that the laser beam stayed within the phase selected and did not penetrate inclusions.

Fresh calcite samples were selected from carbonatites for isotopic analyses. The mineral samples were crushed down to grains of 1 mm in size, sieved and washed, then handpicked for analyses. The carbon and oxygen isotopic compositions of the calcites were measured at the Institute of Geochemistry, Chinese Academy of Sciences using a continuous-flow isotope ratio mass spectrometer (Iso-Prime). Analytical error is ±0.1‰ for both carbon and oxygen, and the results are expressed conventionally as the per mille (‰) variation relative to SMOW and PDB, respectively. For Sr isotopic analyses, fresh calcite mounted in a polished epoxy mount with calcite core exposed. The analyses were performed with a Neptune LA-MC-ICPMS at the Australian National University. Two or three calcite grains from the same whole rock were repeatedly measured. The spot diameters used to measure these samples and standard were 178 and 233 μm, respectively. The average $^{87}Sr/^{86}Sr$ ratio obtained for the Tridacna

standard was 0.70913, whose accepted value within the laboratory is 0.70917.

4. Results

4.1. Element geochemistry

Concentrations of major and trace elements of carbonatites from HYC, QLT and HLP are summarized in Table 1 and plotted on a primitive mantle normalized diagram in Fig. 3. Results of the LA-ICPMS analyses are given in Table 2. Fig. 4 shows the chondrite-normalized solution ICP REE patterns for whole rock and laser ICP-MS analyses of calcite crystals.

The carbonatites from the three locations contain low alkalis, and are typical calciocarbonatites (Woolley and Kempe, 1989), with CaO/(CaO+MgO+FeO+MnO) ratios of 93.6–98.7%.

General features of the geochemistry of the carbonatite dykes from Fig. 3 are similar, with relative enrichment in Ba, U, Pb, Sr and depletion in Zr and Hf relative to adjacent elements on the mantle normalized plot. They are characterized by lower Rb and Nb, higher Y and Yb and similar Sr, and Ba, LREE (La–Nd; except for the QLT sample) contents with respect to the compositions of typical calciocarbonatites (Woolley and Kempe, 1989). Note that the HREE contents of these carbonatite samples are high (e.g. Yb>30 ppm), much higher than any previously analyzed sample from a carbonatite (Figs. 3, 4A). They have flat to slightly LREE enriched patterns with La/Yb_n=2.0–4.9, 1.0–5.5, 1.3 for HYC, HLP and QLT, respectively and negligible Eu anomalies (Fig. 4). A review of the REE in carbonatites is given by Cullers and Graf (1984), who point out that carbonatites contain the highest contents of REE and highest LREE/HREE ratios of any igneous rocks. This conclusion is supported by almost all research on carbonatites (Nelson et al., 1988; Hornig-Kjarsgaard, 1998; and references therein). It is obvious that the REE geochemical characteristics of these carbonatite dykes from the Lesser Qinling are unique in that they do not show the expected LREE enrichment.

The Zr, Nb, Ta, Th and U contents from the calcite crystals in these carbonatite samples are below detection limits of the LA-ICPMS. They have lower Rb, Ba, but similar Sr, Y, Pb concentrations to the whole rocks. Systematic differences between core and rim compositions have been noted, especially in HYC. The LREE contents gradually decrease from core to rim, but the HREE abundances are constant. There are no systematic changes for Sr or Y from core to rim (Table 2 online). Importantly, the core shows similar REE concentration and pattern to the whole rock (Fig. 4). The calcite crystal analyses show smooth LA-ICPMS profiles for the REE, with no sign of inclusions.

4.2. C–O and Sr isotopic geochemistry

Data for carbon, oxygen and strontium isotopic analyses are given in Table 3. The carbon isotopic composition of calcite lies within a narrow range between −6.75 and −7.01‰ $\delta^{13}C$, and the oxygen isotopic composition varies slightly between 7.61 and 9.48‰ $\delta^{18}O$. These values lie within the primary, mantle-derived carbonatite field as defined by Keller and Hoefs (1995).

The present day Sr isotopic ratios for the calcite samples are considered to approximate initial ratios because of the relatively young age of the carbonatite (181 Ma) and very low Rb/Sr ratios (Tables 2 and 3). The $^{87}Sr/^{86}Sr$ ratios from the three locations are similar (0.70495–0.70530, 0.70480–0.70557, 0.70546 for HYC, HLP and QLT, respectively). These values are close to the value expected for EM1 mantle composition. The high Sr contents and low Rb/Sr ratios of the calcites make it likely that the Sr isotopic values of the calcites accurately reflect the composition of the carbonatite

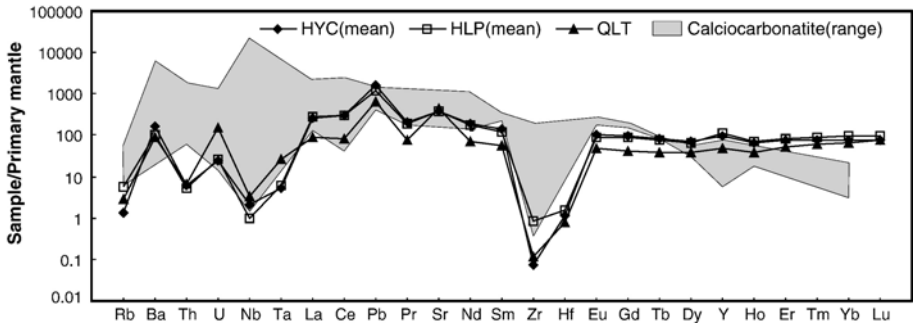

Fig. 3. Primitive mantle-normalized trace element abundances of carbonatites. U content of HYC-9 was omitted for calculating the mean. The data for calciocarbonatite are from Woolley and Kempe (1989). Normalization values from Sun and McDonough (1989).

Table 2
LA-ICPMS analyses of calcite cores

Samples	HYC-5-1	HYC-5-2	HYC-5-3	HYC-5-4	HYC-7-1	HYC-7-2	HYC-7-3	HYC-10-1	HYC-10-2	HYC-10-3	HYC-10-4	HYC-13-1	HYC-13-2	HYC-13-3	HYC-13-4	HYC-20-1	HYC-20-2	HYC-20-3	HYC-20-4
Rb	0.11	0.09	0.09	0.09	0.09	0.08	0.12	0.07	0.08	0.07	0.07	0.07	0.07	0.09	0.06	0.10	0.10	0.10	0.09
Ba	5.36	4.90	5.14	–	4.55	7.94	–	5.48	4.63	6.47	6.94	5.50	–	6.69	4.80	5.17	–	9.53	8.41
Pb	107	102	102	69.4	108	56.0	132	103	96.8	110	102	119	82.4	114	139	103	109	59.3	62.3
Sr	6396	6014	5949	6460	6639	6670	7050	7125	7844	7264	6568	6834	6671	8606	6707	7025	7184	6351	6370
Y	348	320	304	311	305	289	289	211	214	228	235	266	265	258	234	335	303	325	332
La	154	130	104	104	163	62.7	159	211	176	212	188	83.1	69.5	169	63.8	108	112	64.0	52.1
Ce	380	368	281	315	407	232	413	369	310	408	388	275	214	394	209	294	292	210	189
Pr	49.4	50.0	37.8	43.9	54.5	37.8	55.5	43.1	36.2	48.2	47.1	42.3	33.1	51.0	33.4	41.6	39.3	33.0	31.3
Nd	224	231	178	210	246	189	241	187	164	209	205	200	161	215	164	210	190	176	174
Sm	51.1	51.3	40.6	50.3	56.1	49.6	52.0	37.3	35.2	40.5	39.8	44.0	40.1	43.7	37.6	54.7	45.8	49.7	50.9
Eu	13.1	13.0	10.2	13.0	14.9	13.5	13.9	8.70	7.92	9.21	9.59	11.4	10.8	11.6	9.78	14.3	12.2	13.4	13.7
Gd	47.9	47.6	38.7	47.2	53.3	48.2	46.1	31.7	31.0	34.2	34.3	40.7	38.7	38.6	34.0	53.8	45.2	50.0	51.3
Tb	7.51	7.28	6.14	7.32	8.36	7.59	7.23	4.60	4.56	5.01	5.08	6.16	6.08	5.97	5.24	8.23	7.03	7.80	7.92
Dy	48.8	46.4	41.2	46.2	50.5	45.4	43.5	29.2	29.4	32.0	32.5	37.9	38.2	37.3	32.3	51.2	44.1	49.0	49.9
Ho	10.50	9.70	9.14	9.48	10.5	9.60	9.60	6.41	6.53	7.08	7.26	8.52	8.45	8.17	7.33	10.2	9.19	9.91	10.03
Er	33.8	30.4	31.4	29.2	30.4	28.8	29.4	21.1	21.7	23.5	24.3	26.7	26.0	25.7	23.1	30.6	27.8	29.7	30.0
Yb	39.6	35.1	39.5	33.2	34.3	32.8	34.9	26.2	27.1	30.2	31.5	31.5	31.5	31.3	27.8	34.1	32.1	33.6	33.6
Lu	5.28	4.66	5.63	4.40	4.95	4.80	5.25	3.79	3.94	4.53	4.58	4.59	4.60	4.55	4.09	4.68	4.48	4.59	4.55
La/Yb_n	2.64	2.52	1.79	2.14	3.22	1.30	3.09	5.48	4.41	4.76	4.06	1.80	1.50	3.66	1.56	2.15	2.37	1.29	1.05
Gd/Yb_n	0.98	1.10	0.79	1.15	1.26	1.19	1.07	0.98	0.93	0.92	0.88	1.05	0.99	1.00	0.99	1.28	1.14	1.20	1.23
δCe	0.81	0.80	0.79	0.81	1.05	1.16	1.06	0.77	0.73	0.75	0.79	1.12	1.08	1.03	1.10	0.80	0.82	0.82	0.82
δEu	1.05	1.11	1.08	1.13	0.83	0.84	0.86	0.94	0.94	0.98	1.00	0.82	0.83	0.86	0.83	1.06	1.06	1.11	1.13

Samples	HLP-1-1	HLP-1-2	HLP-1-3	HLP-1-4	HLP-3-1	HLP-3-2	HLP-3-3	HLP-3-4	HLP-6-1	HLP-6-2	HLP-6-3	HLP-6-4	HLP-6-5	HLP-6-6	QLT-1-1	QLT-1-2	QLT-1-3	QLT-1-4	QLT-1-5	QLT-1-6
Rb	0.10	0.09	0.09	0.11	0.12	0.14	0.12	0.12	0.24	0.09	0.08	0.15	0.10	0.14	Bdl	Bdl	Bdl	0.13	Bdl	Bdl
Ba	36.4	39.2	48.7	45.0	42.8	24.0	33.6	42.8	23.5	39.2	36.5	40.7	35.6	95.2	30.3	59.9	50.5	49.2	42.6	33.0
Pb	44.7	43.7	47.2	46.5	52.7	66.4	56.5	58.7	66.3	56.2	53.6	58.2	53.2	96.5	64.1	70.5	75.6	72.2	70.9	68.3
Sr	6534	6864	6558	6789	6179	6722	5905	6043	6425	6443	6109	5986	5836	5634	5754	5861	5971	8960	9129	8508
Y	261	258	268	266	367	423	335	425	547	312	304	416	423	549	213	156	147	172	154	159
La	180	245	206	193	126	152	124	144	150	126	116	141	128	160	34.5	35.5	38.2	42.1	45.5	45.1
Ce	417	514	486	438	314	444	309	367	424	295	275	343	318	412	89.0	75.7	82.0	90.0	96.7	100
Pr	54.1	62.6	61.7	55.8	42.0	65.4	41.4	50.7	65.4	31.0	37.4	48.6	44.5	57.6	12.7	9.69	10.5	11.6	12.0	12.8
Nd	234	265	267	241	201	325	197	249	343	182	170	230	212	264	62.9	43.5	46.8	51.9	53.1	56.5
Sm	46.1	50.5	50.7	46.9	46.5	74.4	45.7	59.5	90.6	42.2	39.6	54.5	51.8	61.1	17.2	10.4	10.7	12.4	11.6	12.4
Eu	11.4	11.9	13.0	12.0	12.1	19.2	11.9	15.4	24.8	11.1	10.7	14.7	13.7	16.2	5.58	3.87	3.52	4.08	3.88	3.93
Gd	39.1	40.7	42.2	39.8	45.4	67.1	44.1	57.0	89.0	39.8	38.1	54.1	52.4	58.8	19.4	12.4	11.4	13.5	11.7	12.9
Tb	5.83	5.82	6.20	5.84	6.95	9.67	6.68	8.59	13.5	6.30	6.02	8.40	8.18	9.63	3.46	2.14	1.96	2.42	1.93	2.08
Dy	36.0	35.8	37.9	36.1	46.4	60.3	43.4	56.2	81.7	41.1	39.0	55.4	53.7	63.4	24.8	15.8	14.4	17.2	14.0	14.4
Ho	8.19	8.15	8.50	8.27	10.9	13.2	10.1	12.9	18.0	9.64	9.30	12.9	13.2	15.6	6.33	4.34	3.72	4.60	3.62	3.73
Er	25.8	25.9	27.0	26.4	37.8	41.9	34.3	43.0	54.6	31.8	30.8	42.0	44.4	51.6	22.4	15.9	13.4	17.0	13.6	13.3
Yb	32.1	31.8	33.6	31.9	50.2	50.3	45.9	56.4	64.7	42.9	42.1	55.0	62.2	68.3	32.6	25.8	22.3	27.4	22.5	21.7
Lu	4.67	4.60	4.98	4.56	7.21	7.13	6.66	8.10	9.35	6.62	6.52	8.11	9.39	9.50	5.02	4.27	3.70	4.45	3.72	3.60
La/Yb_n	3.80	5.23	4.17	4.10	1.70	2.05	1.84	1.74	1.58	2.00	1.88	1.74	1.39	1.59	0.72	0.94	1.17	1.05	1.37	1.42
Gd/Yb_n	0.99	1.03	1.02	1.01	0.73	1.08	0.78	0.82	1.11	0.75	0.73	0.80	0.68	0.70	0.48	0.39	0.41	0.40	0.42	0.48
δCe	1.02	1.00	1.04	1.02	0.80	0.83	0.81	0.81	1.03	1.01	1.01	1.00	1.02	1.04	1.03	0.99	0.99	0.99	1.00	1.01
δEu	0.82	0.80	0.86	0.85	1.05	1.08	1.04	1.04	0.84	0.82	0.84	0.83	0.80	0.82	0.93	1.04	0.97	0.96	1.02	0.95

Bdl, below detection limit;-, affected by inclusion.

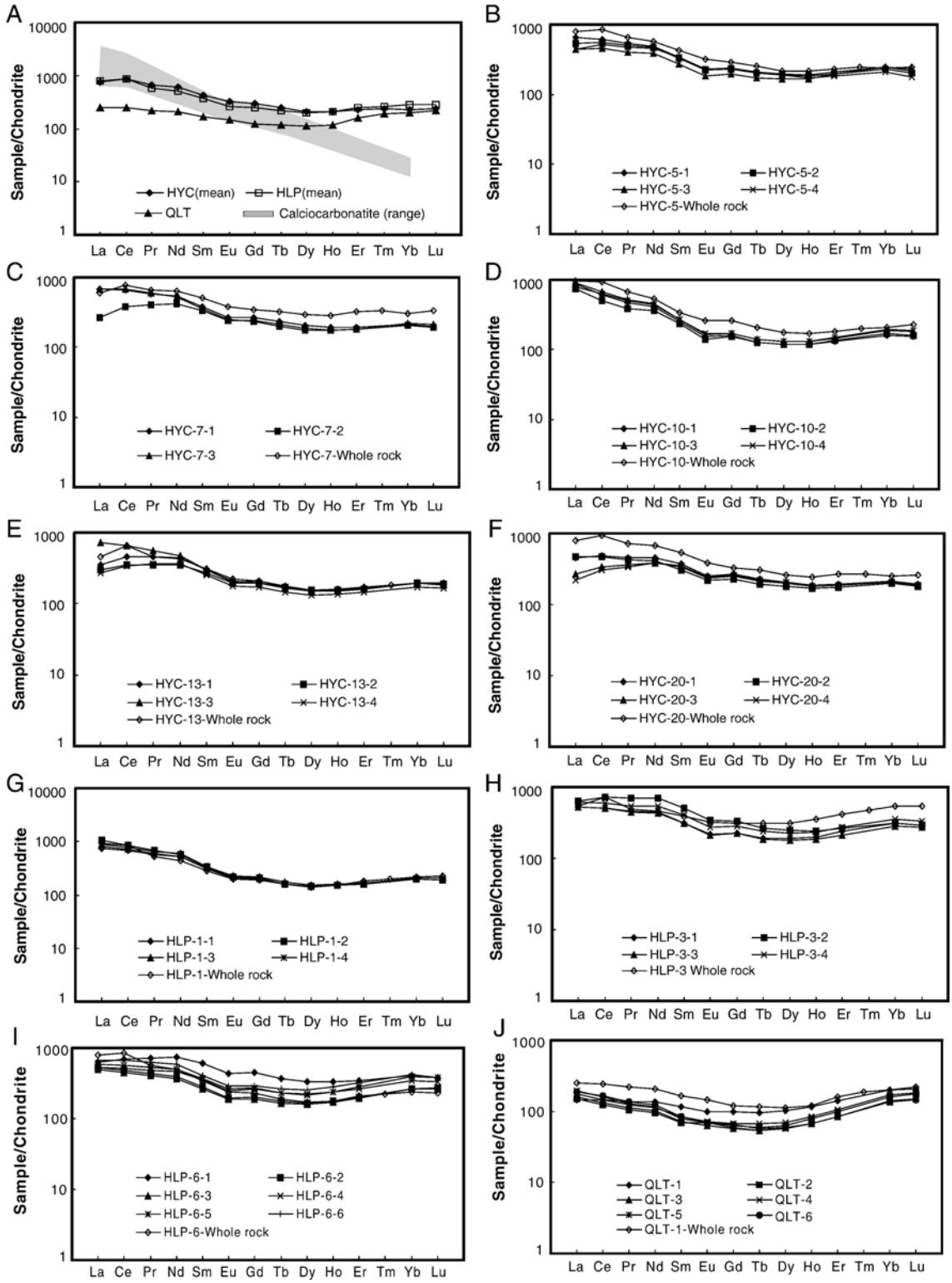

Fig. 4. Chondrite-normalized REE concentrations of carbonatite whole rocks and calcite cores. A, carbonatite whole rocks only; B, C, D, E, F, G, H, I, J, representative calcite cores and whole rock for the same sample. The data for calciocarbonatite are from Woolley and Kempe (1989). Normalization values from McDonough and Sun (1995).

Table 3
C, O and Sr isotopic contents of calcites

Sample	HYC-7	HYC-10	HYC-13	HYC-14	HYC-20	HLP-1	HLP-2	HLP-3	HLP-5	QLT-1
$\delta^{13}C_{PDB}$ (‰)	−6.84	−7.0	−6.86	−7.01	−6.78	−6.92	−6.81	−6.75	−6.76	−6.93
$\delta^{18}O_{SMOW}$ (‰)	8.33	7.85	8.04	7.61	8.44	9.27	9.48	8.69	8.81	8.99
$^{87}Sr/^{86}Sr$	0.70496±2	0.70536±2	0.70489±2	0.70496±2	0.70524±2	0.70475±6	0.70498±3	0.70571±2	0.70509±2	0.70548±2
	0.70496±2	0.70525±2	0.70512±2	0.70494±2	0.70527±2	0.70483±4	0.70503±4	0.70544±2	0.70555±2	0.70545±20
						0.70481±33	0.70513±3			
Mean	0.70496	0.70530	0.70501	0.70495	0.70525	0.70480	0.70505	0.70557	0.70532	0.70546
$^{87}Rb/^{86}Sr$	0.0008	0.0005	0.0003	0.0001	0.0002	0.0011	0.0040	0.0004	0.0001	0.0006
$(^{87}Sr/^{86}Sr)_0$	0.70496	0.70530	0.70501	0.70495	0.70525	0.70480	0.70504	0.70557	0.70532	0.70546

$^{87}Rb/^{86}Sr$ ratio was calculated using the Rb and Sr abundances measured by solution ICPMS. Initial $^{87}Sr/^{86}Sr$ ratio was calculated assuming emplacement age of 180 Ma.

magma, which in turn the composition of the carbonatite mantle source.

5. Discussion

Why do the Lesser Qinling carbonatites show flat to slightly LREE enrichment patterns, and especially why do they have unusually high HREE concentrations, in contrast with all other carbonatites? Do these carbonatite dykes represent melts derived directly from the mantle, are they the products of fractional crystallization or are they an immiscible liquid from that separated a carbonated silicate melt? The C and O isotopic compositions are consistent with primary mantle-derived carbonatites, and there is no evidence to suggest that they have been affected by secondary hydrothermal alteration of a type that may have led to loss of LREE. It is generally accepted that carbonatite parental magmas are generated by extremely low degrees of partial melting of a carbonated peridotitic or eclogitic source and that they are therefore likely to have high abundances of incompatible trace elements. Their strong LREE enrichment relative to HREE is generally attributed to garnet remaining in the source region following melting. Table 4 shows the estimates for La and Yb of bulk peridotite or eclogite/carbonatite partition coefficients (lherzolite with and without garnet and/or amphibole). The higher partition coefficients for Yb than for La and $D_{Yb/La}$ ranging from 21 to 158 mean that moderate to extreme fractionation of La from Yb is expected to occur if carbonatites form by low degrees of partial melting of lherzolite or eclogite, respectively. Besides, primary carbonatites are characterized by elevated Mg-numbers (Sweeney, 1994), high Mg+Fe/Ca ratios, moderate amounts of alkalis (Eggler, 1989) and must have compositions dominated by calcic dolomite (Lee and Wyllie, 1998). The experimental evidence suggests that calciocarbonatites can be generated through the reaction of primary, mantle-derived Mg-rich carbonatite melts with harzburgitic or lherzolitic assemblages at pressures that are lower than the carbonatite source region (Dalton and Wood, 1993). This will inevitably lead to further fractionation of LREE to HREE because Yb is more compatible than La (Table 4). Reaction of a primary carbonatite melt with harzburgite or lherzolite cannot therefore explain the low La/Yb_n ratios seen in the Lesser Qinling samples. Similarly, trace element partitioning between immiscible silicate–carbonate liquid systems cannot be the answer because LREE partition into the carbonate liquid, whereas HREE partition preferentially into the silicate melt (Veksler et al., 1998a,b). Finally, typically fractional crystallization-derived calciocarbonatites like those from Kovdor, Kola Peninsular, Russia, also

Table 4
Average partition coefficients for olivine, clinopyroxene, orthopyroxene, garnet, amphibole in equilibrium with a carbonatite melt, and calculated bulk partition coefficients for a carbonatite source

Mineral	Ol	Cpx	Opx	Gar	Amph	Bulk *D* gar. lherz	Bulk *D* sp. Lherz	Bulk *D* amph. Lherz	Bulk *D* eclogite
D_{La}	–	0.051	0.005	0.0014	0.01	0.007	0.010	0.008	0.026
D_{Yb}	0.03	1.0	0.073	7.2	0.16	0.447	0.214	0.165	4.1
$D_{Yb/La}$						63.8	21.4	20.6	158

Ol, olivine; cpx, clinopyroxene; opx, orthopyroxene; gar, garnet; amp, amphibole. Data source: Adam and Green (2001), Blundy and Dalton (2000; experiment DC15), Salters et al. (2002; experiment RD1097-8), Bizimis et al. (2003). Because of the scarcity of La partition coefficient in orthopyroxene, Ce is used is as a proxy for La. A dash (–) denotes below detection. Mineral modes are estimated from Bizimis et al. (2003) and Yaxley and Brey (2004): garnet lherzolite: ol=0.60, opx=0.20, cpx=0.12, gar=0.04, amph=0.04; spinel lherzolite: ol=0.60, opx=0.22, cpx=0.18, gar=0, amph=0; amphibole–spinel lherzolite: ol=0.60, opx=0.20, cpx=0.12, gar=0, amph=0.08; eclogite: cpx=0.50, gar=0.50.

have steep REE patterns (La/Yb_n>40; Verhulst et al., 2000). There, the crystallization sequence of the carbonatite complex, form a concentric zonation with cross-cutting pods and dykes of calciocarbonatite. No such rock complex was observed in the Qinling dykes, but this may be the result of the present exposure level.

The calcites from the Lesser Qinling carbonatite dykes show similar Sr isotopic compositions to EM1, but their REE patterns are obviously different to that of EM1 derived magmas, which are LREE enriched (Hofmann, 1997). The combined Sr, Nd and Pb isotopic compositions from the East African Rift suggest mixing between a HIMU- and EM1-type mantle components play a major role in the genesis of carbonatites and related silicate rocks in this region (e.g. Bell and Blenkinsop, 1987; Bell and Simonetti, 1996). Bell and Tilton (2001) suggest that the EM1–HIMU mixing reflects the heterogeneous nature of a mantle plume that carries both these components from deep in the mantle. However, the available partition coefficients between peridotite/eclogite and carbonatite melt (Table 4) cannot generate the flat to slightly LREE enrichment carbonatite from a normal mantle source that includes components of EM1- and HIMU-type mantles. Both are thought to be enriched in LREE relative to the primary mantle (Hofmann, 1997). The DMM (N-type MORB mantle), characterized by depletion of LREE, is an alternative source for the primary carbonatite magmas, but is likely to be dolomitic. More importantly, the relatively radiogenic initial Sr isotopic compositions of these calcites can be used to rule out a significant DMM component in the Lesser Qinling source region.

It is difficult to reconcile the nearly flat REE patterns of the Lesser Qinling carbonatites with a primary magmatic origin. Their $CaCO_3$ content is too high to represent a calciocarbonatite magma generated after metasomatism of wall rock lherzolite, which produce carbonate liquids containing no more than 75–87% $CaCO_3$ (Dalton and Wood, 1993; Wyllie and Lee, 1998). Furthermore, concentrations of all of the REE in the bulk rock and calcite are similar. The carbonatite compositions can only represent the parental magma if the calcite/melt partition coefficients (*D*) of all REE are ~ 1 for, which is unlikely.

An alternative explanation is that the carbonatite dykes represent calcite-rich cumulate that has crystallized from a carbonatite melt. Calcite crystals are known to sink rapidly and separate from their low viscosity host carbonate magma (Wyllie and Tuttle, 1960). More likely, in the case of the Lesser Qinling carbonatite dykes, the carbonate crystals grew inward from the walls of a flowing carbonatite dyke. The carbonates have a high modal abundance of calcite with high REE contents (Table 3), and it is apparent that their REE content controls the REE abundance in the bulk rock. Analyses of carbonates by LA-ICPMS from other

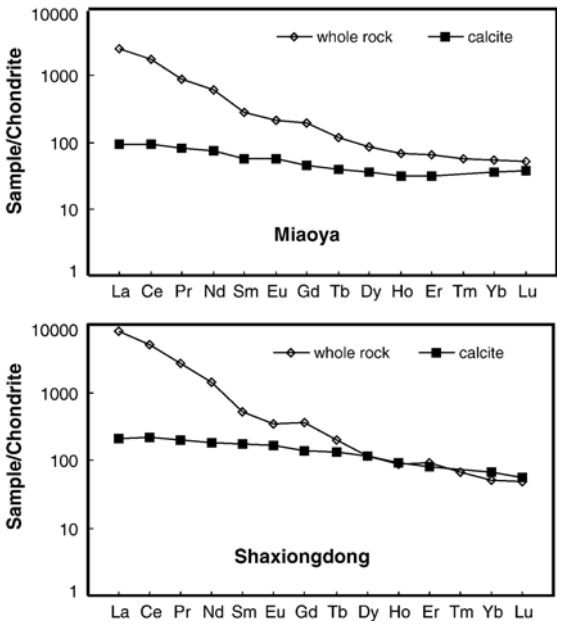

Fig. 5. Chondrite-normalized REE concentrations of carbonatites and cores in calcite crystals from Miaoya and Shaxiongdong in China. The data are not published. Normalization values from McDonough and Sun (1995).

calciocarbonatites also show essentially flat to slightly LREE enrichment patterns, even though the associated carbonatite is strongly LREE enriched (Fig. 5). This requires the calcite/melt D across REE vary systematically with ionic radius such that the D decrease with increasing ionic radius so that calcite/melt D for HREE are higher than for the LREE. Thus, a LREE enriched carbonatite can crystallize carbonates with approximately flat patterns, and a carbonate cumulate can have a flat REE pattern if it contains little trapped liquid. Variation in the slope of REE patterns in carbonatites, between chondritic and strongly LREE enriched, can be produced by mixing variable amounts of melts and carbonate crystals.

Many researchers consider that carbonatites were derived by small degrees of melting ($< \approx 1\%$) of a garnet-rich eclogitic source (Nelson et al., 1988; Hoernle et al., 2002; Yaxley and Brey, 2004), for example CO_2- and volatile-rich subducted oceanic crust (eclogite). Under these circumstances, the extreme LREE enrichment and low HREE abundances of carbonatites may be a primary magmatic feature. However, the model is not feasible for the Lesser Qinling carbonatites, which have high HREE contents that imply the primary magma contained similar or higher HREE abundances. The D_{Yb} for a garnet-rich source is 0.447–4.1 (Table 4). A garnet-rich source region can only produce a carbonatite melt with Yb > 30 ppm if it contained Yb > 12. No known mantle source region contains this much Yb (e.g. McDonough and Sun, 1995). The nature of the mantle source region for the Lesser Qinling carbonatites is not well-constrained but it may have been garnet-poor.

6. Conclusions

The following conclusions can be drawn from this work:

1. The REE distribution in the Qinling carbonatites is controlled by that of calcites because of their high modal amounts. These rocks show flat to slightly LREE enriched chondrite-normalized patterns, which do not represent the compositions of the carbonatite parental magmas. They formed by the accumulation of calcites along the walls of a conduit through which a carbonatite magma was moving.
2. The Qinling carbonatites may evolve from a garnet-poor source region, which led to their HREE enrichment.

Acknowledgments

We thank Dr. M.F. Zhou for supporting the trace element analysis, N. An and L. Kinsley for the assistance with the isotopic analytical work. We also thank Prof. X.H. Yu for discussion and two anonymous reviewers for reviewing and improving the manuscript. This research was financially supported by the Chinese National Science Foundation (No. 40303004), the President Scholarship of the Chinese Academy of Sciences to C. Xu, and CAS grant KZCX3-SW-124.

Appendix A. Supplementary data

Supplementary data associated with this article can be found, in the online version, at doi:10.1016/j.lithos.2006.07.016.

References

Adam, J., Green, T., 2001. Experimentally determined partition coefficients for minor and trace elements in peridotite minerals and carbonatitic melt, and their relevance to natural carbonatites. Eur. J. Mineral. 13, 815–827.

Bell, K., 1998. Radiogenic isotope constraints on relationships between carbonatites and associated silicate rocks — a brief review. J. Petrol. 39, 1987–1996.

Bell, K., Blenkinsop, J., 1987. Nd and Sr isotopic composition of East African carbonatites: implications for mantle heterogeneity. Geology 15, 99–102.

Bell, K., Simonetti, A., 1996. Carbonatite magmatism and plume activity: implications from the Nd, Pb and Sr isotope systematics of Oldoinyo Lengai. J. Petrol. 37, 1321–1339.

Bell, K., Tilton, G.R., 2001. Nd, Pb, and Sr isotopic compositions of East African carbonatites: evidence for mantle mixing and plume inhomogeneity. J. Petrol. 42, 1927–1945.

Bizimis, M., Salters, V.J.M., Dawson, J.B., 2003. The brevity of carbonatite source in the mantle: evidence from Hf isotopes. Contrib. Mineral. Petrol. 145, 281–300.

Blundy, J., Dalton, J., 2000. Experimental comparison of trace element partitioning between clinopyroxene and melt in carbonate and silicate systems, and implications for mantle metasomatism. Contrib. Mineral. Petrol. 139, 356–371.

Cullers, R.L., Graf, J.L., 1984. Rare earth elements in igneous rocks of the continental crust: predominantly basic and ultrabasic rocks. In: Henderson, P. (Ed.), Developments in Geochemistry. Rare earth geochemistry, Vol. 2. Elsevier, Amsterdam, pp. 237–274.

Dalton, J.A., Wood, B.J., 1993. The compositions of primary carbonate melts and their evolution throng wallrock reaction in the mantle. Earth Planet. Sci. Lett. 119, 511–525.

Eggler, D.H., 1989. Carbonatites, primary melts, and mantle dynamics. In: Bell, K. (Ed.), Carbonatites: Genesis and Evolution. Unwin Hyman, London, pp. 561–579.

Harmer, R.E., 1999. The petrogenetic association of carbonatite and alkaline magmatism: constraints from the Spitskop complex, South Africa. J. Petrol. 40, 525–548.

Harmer, R.E., Gittins, J., 1998. The case for primary, mantle-derived carbonatite magma. J. Petrol. 39, 1895–1903.

Hofmann, A.W., 1997. Mantle geochemistry: the message from oceanic volcanism. Nature 385, 219–229.

Hoernle, K., Tilton, G., Le Bas, M.J., Duggen, S., Garbe-Schonberg, D., 2002. Geochemistry of oceanic carbonatites compared with

continental carbonatites: mantle recycling of oceanic crustal carbonate. Contrib. Mineral. Petrol. 142, 520–542.
Hornig-Kjarsgaard, I., 1998. Rare earth elements in sovitic carbonatites and their mineral phases. J. Petrol. 39, 2105–2121.
Keller, J., Hoefs, J., 1995. Stable isotope characteristics of recent natrocarbonatites from Oldoinyo Lengai. In: Bell, K., Keller, J. (Eds.), Carbonatites Volcanism: Oldoinyo Lengai and Petrogenesis of Natrocarbonatites. LAVCEI Proceeding in Volcanology. Springer-Verlag, Berlin, pp. 113–123.
Kjarsgaard, B.A., Hamilton, D.L., 1989. The genesis of carbonatites by immiscibility. In: Bell, K. (Ed.), Carbonatites: Genesis and Evolution. Unwin Hyman, London, pp. 388–404.
Le Bas, M.J., 1989. Diversification of carbonatites. In: Bell, K. (Ed.), Carbonatites: Genesis and Evolution. Unwin Hyman, London, pp. 428–447.
Lee, W.J., Wyllie, P.J., 1997a. Liquid immiscibility between nephelinite and carbonatite from 1.0 to 2.5 Gpa compared with mantle composition. Contrib. Mineral. Petrol. 127, 1–6.
Lee, W.J., Wyllie, P.J., 1997b. Liquid immiscibility in the join of Na–$AlSiO_4$–$NaAlSi_3O_8$–$CaCO_3$ at 1 GPa: implications for crustal carbonatites. J. Petrol. 38, 1113–1135.
Lee, W.J., Wyllie, P.J., 1998. Petrogenesis of carbonatite magmas from mantle to crust, constrained by the system CaO–(MgO–FeO*)–(NaO+K_2O)–(SiO_2+Al_2O_3+TiO_2)–CO_2. J. Petrol. 39, 495–517.
Longerich, H.P., Jackson, S.E., Gunter, D., 1996. Laser ablation inductively coupled plasma mass spectrometric transient signal data acquisition and analyze concentration calculation. J. Anal. At. Spectrom. 11, 899–904.
McDonough, W.F., Sun, S.S., 1995. The composition of the Earth. Chem. Geol. 120, 223–253.
Meng, Q.R., Zhang, G.W., 2000. Geologic framework and tectonic evolution of the Qinling orogen, central China. Tectonophysics 323, 183–196.
Nelson, D.R., Chivas, A.R., Chappell, B.W., McCulloch, M.T., 1988. Geochemical and isotopic systematics in carbonatites and implications for the evolution of ocean–island sources. Geochim. Cosmochim. Acta 52, 1–17.
Qi, L., Hu, J., Gregoire, D.C., 2000. Determination of trace elements in granites by inductively coupled plasma mass spectrometry. Talanta 51, 507–513.
Ratschbacher, L., Hacker, B.R., Calvert, A., Webb, L.E., Grimmer, J. C., McWilliams, M.O., Ireland, T., Dong, S.W., Hu, J.M., 2003. Tectonic of the Qinling (Central China): tectonostratigraphy, geochronology, and deformation history. Tectonophysics 366, 1–53.
Salters, V.J.M., Longhi, S., Bizimis, J.E., 2002. Near mantle solidus trace element partitioning at pressures up to 3.4 GPa. Geochem. Geophys. Geosyst. 3. doi:10.1029/2001GC000148.
Sun, S.S., McDonough, W.F., 1989. Chemical and isotopic systematics of oceanic basalt: implications for mantle compositions and processes. In: Saunders, A.D., Norry, M.J. (Eds.), Magmatism in the Ocean BasinsThe Geological Society Spec. Publ., vol. 42, pp. 313–345.
Sweeney, R., 1994. Carbonatite melt compositions in the earth mantle. Earth Planet. Sci. Lett. 128, 259–270.
Veksler, I.V., Nielsen, T.F.D., Sokolov, S.V., 1998a. Mineralogy of crystallized melt inclusions from Gardiner and Kovdor ultramafic alkaline complexes: implications for carbonatites genesis. J. Petrol. 39, 2015–2031.
Veksler, I.V., Petibon, C., Jenner, G.A., 1998b. Trace element partitioning in immiscibility and silicate liquid: an initial experimental study using a centrifuge autoclave. J. Petrol. 39, 2095–2104.
Verhulst, A., Balaganskaya, E., Kirnarsky, Y., Demaiffe, D., 2000. Petrological and geochemical (trace elements and Sr–Nd isotopes) characteristics of the Paleozoic Kovodor ultramafic, alkaline and carbonatite intrusion (Kola Peninsula, NW Russia). Lithos 51, 1–25.
Woolley, A.R., Kempe, D.R.C., 1989. Carbonatites: nomenclature, average chemical composition. In: Bell, K. (Ed.), Carbonatites: Genesis and Evolution. Unwin Hyman, London, pp. 1–14.
Wyllie, P.J., Lee, W.J., 1998. Model system controls on conditions for formation of magesiocarbonatite and calciocarbonatite magmas from the mantle. J. Petrol. 39, 1885–1893.
Wyllie, P.J., Tuttle, O.F., 1960. The system CaO–CO_2–H_2O and the origin of carbonatites. J. Petrol. 1, 1–46.
Xue, F., Lerch, M.F., Kroner, A., Reischmann, T., 1996. Tectonic evolution of the East Qinling Mountains, China, in the Palaeozoic: a review and new tectonic model. Tectonophysics 253, 271–284.
Yaxley, G.M., Brey, G.P., 2004. Phase relations of carbonate-bearing eclogite assemblages from 2.5 to 5.5 GPa: implications for petrogenesis of carbonatites. Contrib. Mineral. Petrol. 146, 606–619.
Yu, X.H., 1992. Geological, mineralogical characteristics and origin of the carbonatites from Huayangchuan, Shanxi Province. Earth Sci. 17, 151–158 (in Chinese with English abstract).